Article

Insights into the Role of Transient Chiral Mediators and Pyridone Ligands in Asymmetric Pd-Catalyzed C–H Functionalization

David E. Hill, Jin-Quan Yu, and Donna G Blackmond

J. Org. Chem., **Just Accepted Manuscript** • DOI: 10.1021/acs.joc.0c01798 • Publication Date (Web): 29 Sep 2020

Insights into the Role of Transient Chiral Mediators and Pyridone Ligands in Asymmetric Pd-Catalyzed C–H Functionalization

David E. Hill,[†,‡] Jin-Quan Yu,[†] Donna G. Blackmond*[†]

[†] Department of Chemistry, The Scripps Research Institute, La Jolla, California 92037, United States

ABSTRACT: Mechanistic investigations uncover a novel role for 2-pyridone ligands and interrogate the origin of enantioselectivity in the (+)-norbornene mediated Pd-catalyzed *meta*-C(aryl)–H functionalization of diarylmethylamines. Observations from kinetic analysis in concert with *in-situ* ^{19}F NMR monitoring allow us to propose that the pyridone ligand plays a role in enhancing the rate- and enantio-determining insertion of an arylpalladium species into a chiral norbornene derivative. The unprecedented features of 2-pyridone ligands in asymmetric 1,2 migratory insertion, and norbornene as a transient chiral mediator in relay chemistry, provide new insights into this ligand scaffold for future developments in stereoselective transition-metal catalyzed C–H functionalization.

INTRODUCTION

Pd-catalyzed C–H functionalization methodologies promoted by 2-pyrdione ligands have become prominent in recent years.[1-9] This class of Pd-catalysis was initially discovered to facilitate norbornene mediated *meta*-C(aryl)–H functionalization[1] and then later developed to perform the Fujiwara–Moritani reaction using the arene substrate as a limiting reagent[5], a long-standing challenge in non-direct C–H activation. Although the norbornene-mediated relay of *ortho*-cyclopalladation to the *meta*-position of an aryl ring system is a well-established process in the Catellani reaction,[10-11] the use of norbornene as a transient chiral mediator to control stereoselectivity in C–H activation is a new approach developed by the Yu group.[7] The origin of the enantioselectivity for this novel stereoselective *meta*-C(aryl)–H functionalization remains speculative. The 2-pyridone ligand scaffold was originally conceived as a potential surrogate in lieu of acetate and was hypothesized to act as an improved internal base for promoting C–H bond cleavage (Scheme 1).[1] Experimental and computational studies of non-directed Pd-3,5-ditrifluoromethyl-2-pyridone-catalyzed C–H functionalization by the Yu group have suggested that the 2-pyridone ligand could accelerate C–H activation by lowering the energy barrier for concerted-metalation deprotonation as well as prevent catalyst degradation by forming a stable trimeric Pd-pyridone complex.[5]

Scheme 1. Role of Pyridone as an Acetate Surrogate in C–H Functionalization.

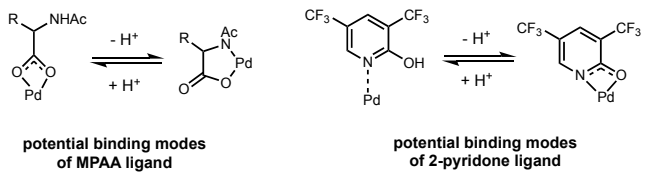

These striking mechanistic features of 2-pyridone ligands and the chiral norbornene transient mediator prompted us to study the reaction in Scheme 2 (conditions from ref. 7), norbornene-mediated Pd-2-pyridone-catalyzed *meta*-C(aryl)–H functionalization. This investigation reports mechanistic studies supporting previous work as well as presenting novel mechanistic understanding of the catalyst resting state and the enantio-controlling step for Pd-catalyzed (+)-norbornene mediated *meta*-C(aryl)–H functionalization. These findings could enable further development of norbornene mediated *meta*-C(aryl)–H functionalization.

Scheme 2: Asymmetric Pd-norbornene (4)-pyridone (5)-catalyzed C–H arylation of diarylmethylamines.

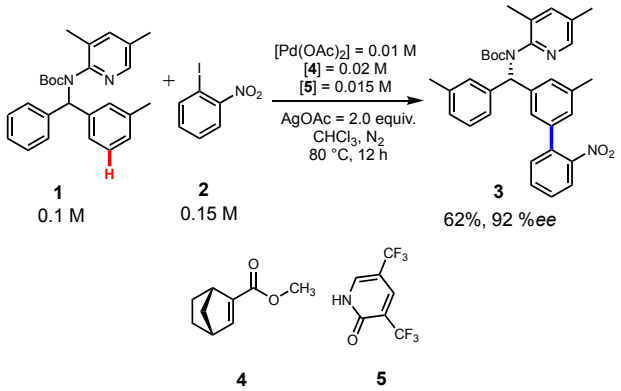

RESULTS AND DISCUSSION

Our mechanistic investigation of the Pd-catalyzed C(aryl)–H arylation of biarylmethylamines (Scheme 2) began with probing the kinetic behavior of the reaction using an aliquot method and HPLC analysis for simultaneous measurement of the consumption of substrate **1** and the formation of reaction product **3**, revealing a temporal loss of reaction mass balance and an increase in % *e.e.* of product **3** from 76% to 90% as the reaction proceeds to high conversion of **1** (Figure 1). Further analysis of the reaction mixture led to the detection of a Pd-norbornene (**4**)-pyridone (**5**)-catalyzed C(aryl)–H double arylation side reaction to yield **7** (Scheme 3). This undesirable process forming **7** accounts for the missing mass and was

hypothesized to occur through the kinetic resolution of product **3** in a second aryl addition. Studies monitoring the reaction of racemic product (±)-**3** yielded a temporal increase in the % e.e. of **3**, from which we calculate that the arylation of **3** to form **7** occurred through a kinetic resolution process with a selectivity factor of s = 7. The Yu group has previous demonstrated chiral norbornenes to facilitate kinetic resolution-based processes; however, the present findings show that two chiral selection steps work in concert to yield the observed high %*ee* product. Thus, two chiral selection steps in sequence result in enantio-enı

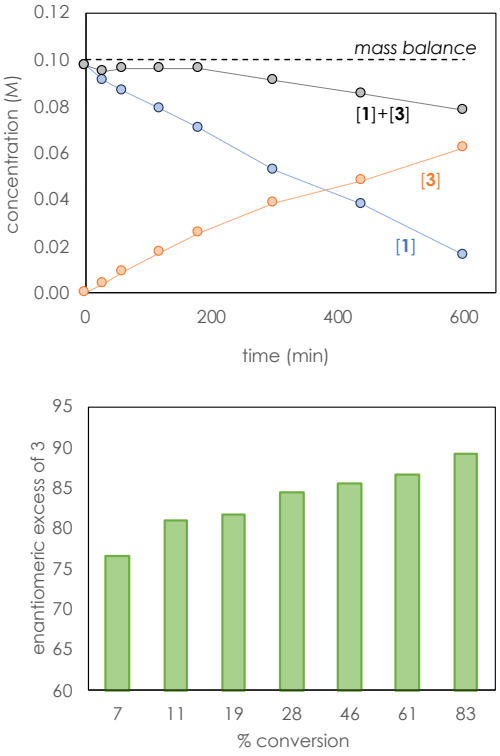

Figure 1: Reaction progress data for reaction of Scheme 2 (top). Temporal monitoring of **3** % *e.e.* (bottom).

Scheme 3. Kinetic Resolution Via Second Arylation of Product 3.

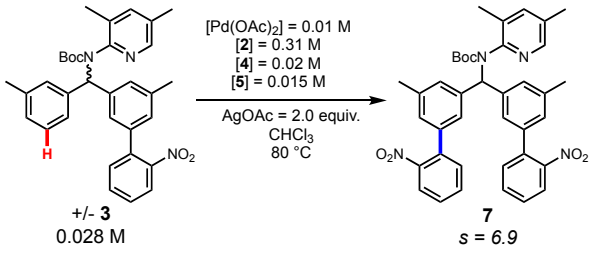

Experiments aimed at determining the catalyst robustness and concentration dependencies of each reaction component were conducted according to the same excess and different excess protocols of Reaction Progress Kinetic Analysis (RPKA)[12-13] with the term "excess" defined by Equation 1. Although the original work included phosphoric acid as an additive, experiments showed that its absence changed neither the enantioselectivity of the reaction nor the global rate of reaction, and therefore it was not added in our kinetic experiments. Figure 2 shows the kinetics profiles for experiments carried out using the same excess protocol. The time-adjusted curves, as indicated by the arrow in Figure 2, enable the comparison of the kinetic profiles for the two experiments as they react under identical substrate conditions onward from the point of intersection of the arrows. The overlay of these two reaction profiles indicates that the reaction rate under standard conditions is not influenced by either the additional catalyst turnovers completed or the presence of products **3** or **7** in the reaction vial, compared to the fresh conditions of the same excess experiment. This observation of overlay for experiments of same excess confirms that the absence of both irreversible catalyst deactivation and product catalyst inhibition during catalysis.

$$[\text{excess}] = [\mathbf{2}]_0 - [\mathbf{1}]_0 \quad (1)$$

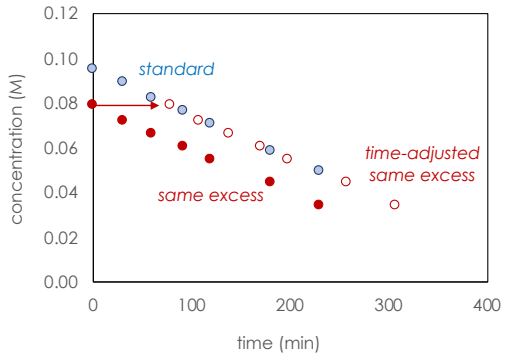

Figure 2: Kinetic profile for C–H arylation reaction shown in Scheme 1 plotted as [**1**] against time carried out using the same excess procedure with [excess] = 0.2 M. Both reactions with $[Pd(OAc)_2]$ = 0.01 M, [**4**] = 0.02 M, [**5**] = 0.015 M, and 3.0 equiv. of AgOAc in chloroform at 80 °C. (blue circles) $[\mathbf{1}]_0$ = 0.1 M; $[\mathbf{2}]_0$ = 0.3 M. (red circles) $[\mathbf{1}]_0$ = 0.08 M; $[\mathbf{2}]_0$ = 0.28 M. (red non-filled circles) time-adjusted data from red circles.

After confirming the robustness of the Pd catalyst, we next interrogated the concentration driving forces of the reaction through different excess experiments. The data for the different excess experiments in Figure 3 demonstrates zeroth order rate dependence for both substrates [**1**] and the [**2**]. First order rate dependence on $[Pd(OAc)_2]$ and [**4**] co-catalyst were revealed via Variable Time Normalization Analysis[14] (Figures 4 and 5). Overlay between the profiles indicates the order in both [Pd] and [**4**] shows n = 1, or first order dependence in each case. We also established the lack of a nonlinear effect on product ee as a function of [**4**].

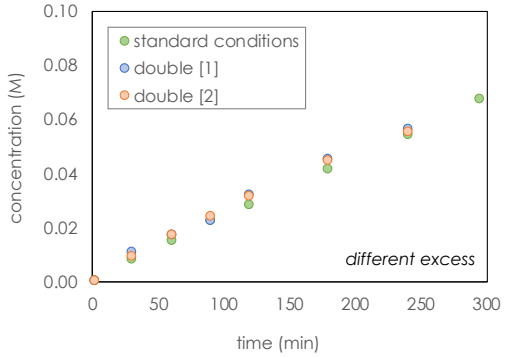

Figure 3: Different excess experiments to determine reaction order in [**1**] and [**2**] plotted as the assumed [**3**] against time. All reactions

with $[Pd(OAc)_2]$ = 0.01 M, [**4**] = 0.02 M, [**5**] = 0.015 M, and 3.0 equiv. of AgOAc in chloroform at 80 °C.

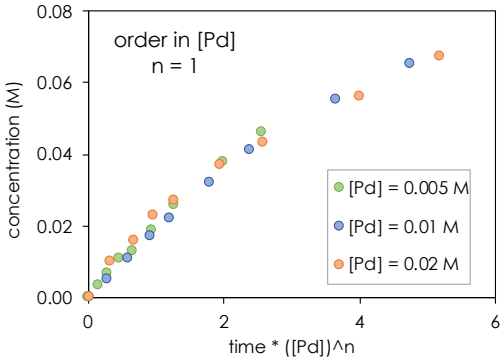

Figure 4: Variable Time Normalization Analysis (VTNA)[14] for reactions containing varied $[Pd(OAc)_2]$ as noted plotted as the assumed [**3**] against normalized-time. All reactions contain [**4**] = 0.02 M, [**5**] = 0.02 M; $[\mathbf{1}]_0$ = 0.1 M; $[\mathbf{2}]_0$ = 0.3 M; and 3.0 equiv. of AgOAc in chloroform at 80 °C. Overlay for n=1 signifies first order kinetics in [Pd].

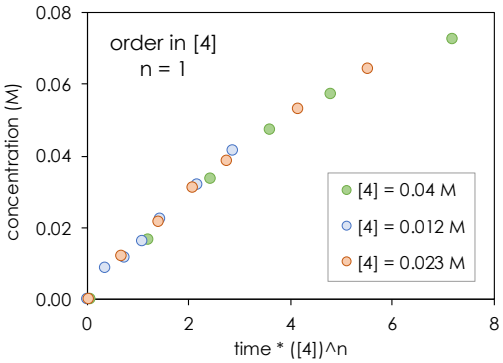

Figure 5: Variable Time Normalization Analysis (VTNA)[14] for reactions containing varied [**4**] plotted as the assumed [**3**] against normalized-time. All reactions contain $[Pd(OAc)_2]$ = 0.01 M, [**5**] = 0.015 M, $[\mathbf{1}]_0$ = 0.1 M; $[\mathbf{2}]_0$ = 0.3 M; and 3.0 equiv. of AgOAc in chloroform at 80 °C.

Figure 6 shows that the initial reaction rate was not dependent on the concentration of pyridone **5**, although at longer reaction times and higher conversion, rate became more sluggish for Pd:[**5**] less than 1:2. This suggests that pyridone plays a role in stabilizing the active catalyst to suppress catalyst deactivation. At concentrations of **5** greater than Pd:[**5**] = 1:3, rate was suppressed which may be due to formation of the multimeric palladium species $Pd_3(\mathbf{5})_5(\mu_2\text{-OH})$ previously characterized by the Yu group[5] and is likely to be a catalytically inactive off-cycle species.

In order to probe the catalyst resting state suggested by the zeroth order rate dependence on [**1**] and [**2**], we carried out ^{19}F NMR reaction monitoring using substrate **1**-F, a derivative of **1** where a fluorine atom replaces the methyl in each of the aryl rings, When substrate **1**-F was combined with $Pd(OAc)_2$ and AgOAc at 50 °C in $CHCl_3$, new ^{19}F NMR signals near -87 ppm and -123 were observed (Figure 7a) that were not associated with either the starting material **1**-F or the arylated or bi-arylated products **3**-F or **7**-F. Adding norbornene and substrate **2** did not change this spectrum (Figure 7b), but addition of pyridone **5** resulted in a shift in the peaks in both regions (Figure 7c). An investigation of the ^{19}F NMR literature[15-20] indicated that the signals located between -84 ppm to -96 ppm could tentatively belong to ortho-palladated aryl fluorides while peaks located between -120 ppm to -125 ppm could potentially indicate the presence of para-palladated aryl fluorides. We suggest that in the absence of **5**, an acetate group serves as a ligand, which may be displaced by **5** (Scheme 4).

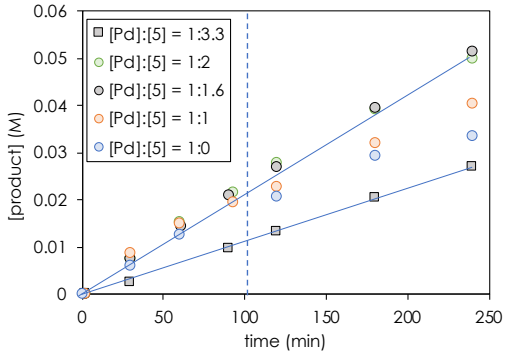

Figure 6: Time course for the reaction of Scheme 2 using different concentrations of pyridone **5** as noted in the legend. $[\mathbf{1}]_0$ = 0.1 M; $[\mathbf{2}]_0$ = 0.3 M; $[Pd(OAc)_2]$ = 0.01 M; [**4**] = 0.02 M; 3.0 equiv. of AgOAc in chloroform at 80 °C.

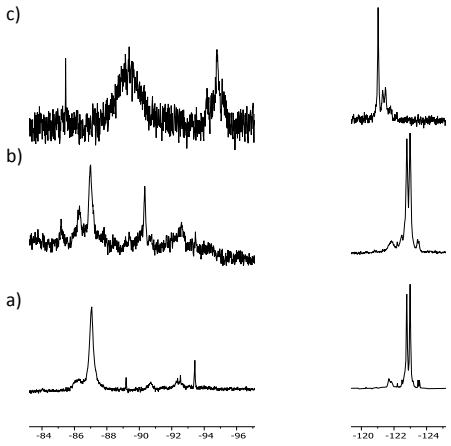

Figure 7: *In-situ* ^{19}F NMR spectroscopy of Pd species observed in reactions with substrate **1**-F. a) interaction of **1**-F with Pd in the absence of both **4** and **5**. b) reaction between **1**-F and **2** in the absence of **5**; c) reaction between **1**-F with **2** in the presence of both **4** and **5**. All reactions were conducted at 50 °C in *d*-$CHCl_3$.

Scheme 4. Putative Pd Species Observed with *via* ^{19}F-NMR.

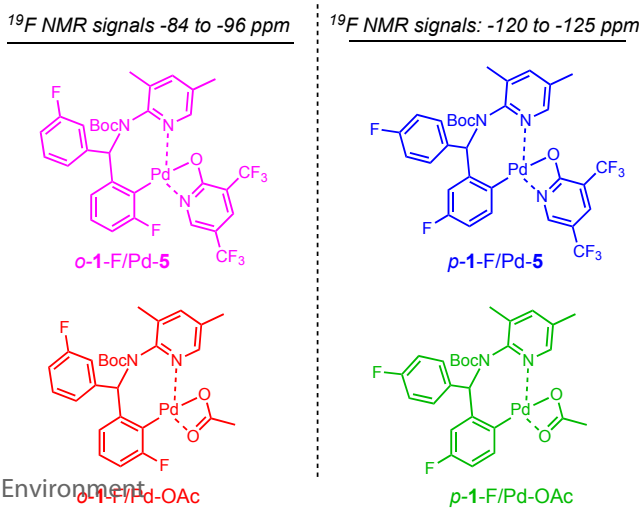

The suggested displacement of an acetate ligand by pyridone **5** is in accordance with our proposal that a species such as *p*-**1**/Pd-**5** is the resting state in the catalytic cycle, with the corresponding *ortho* species forms reversibly off-cycle. In the absence of pyridone **5**, the reaction presumably proceeds through a species such as *p*-**1**/Pd-OAc, with lower enantioselectivity and more rapid catalyst deactivation. Enhanced stabilization of bound substrate by pyridone may also aid in stabilizing the transition state for the migratory insertion of this species into **4**.

The insertion of the racemic arylpalladium intermediate, *p*-**1**/Pd-**5**, into the enantiopure norbornene, **4**, is the first elementary step of the catalytic cycle involving a diasteroselective reaction. The irreversibility of this diasteroselective reaction of *p*-**1**/Pd-**5** with **4** suggests that this rate-determining step is likely to also be the enantio-determining step for the reaction. Interestingly, since the transient chiral mediator **4** only appears in the cycle subsequent to the rate-determining step, any catalytic species containing **4** must be fleeting in concentration.

A recent computational study of this reaction similarly proposed norbornene insertion as the enantiocontrolling step.[21] Protonation of the product-bound species after removal of norbornene was proposed as the rate-determining step, while the original Yu work speculated that oxidative addition of the aryl halide might be rate-determining.[5] Expected concentration dependences would be zero order kinetics in [norbornene] for the mechanism proposed in the computational study, and first order kinetics in [ArX] in the Yu proposal. By contrast, our kinetic investigations, which show first order kinetics in [**5**] and zero order kinetics in [**2**], are not in accord with either suggestion. Our ^{19}F NMR studies taken together with the kinetic dependences support the involvement of both 2-pyridone ligand **4** and norbornene **5** in a single rate- and enantio-determining step.

A reaction mechanism accounting for all of these experimental observations is shown in Scheme 5. The pyridone ligand **5** aids in breaking up the inactive Pd-trimer to bring active catalyst species **8** on-cycle to reversibly react with **1**, forming both the off-cycle intermediate *o*-**1**/Pd-**5** and the active intermediate *p*-**1**/Pd-**5**. This on-cycle arylpalladium species then undergoes rate-determining 1,2-migratory insertion into norbornene, **4**, and the resulting insertion intermediate undergoes oxidative addition of the aryl halide **2**, ultimately yielding product **3**.

CONCLUSION

In summary, our kinetics-based mechanistic investigation has revealed that the 2-pyridone ligand **5** improves the product selectivity and catalyst robustness for the enantio-determining step of insertion of intermediate *p*-**1**/Pd-**5** into the transient chiral mediator, norbornene **4**. We found that stereoselective kinetic resolution of **3** by Pd-**5**-**6**-catalyzed C(aryl)–H arylation contributes to the high % *e.e.* product observed at the end of the reaction. *In-situ* NMR spectroscopy results offer further characterization of the arylpalladium catalyst resting state for this robust Pd-catalyzed (+)-norbornene mediated meta-C(aryl)–H functionalization, supporting its role as a transient chiral mediator. In all previous examples of Pd-catalyzed enantiosetive C-H activation reactions, chiral ligand coordinated to Pd in inducing the chiral transfer in the C-H activation step or the subsequent C-C bond forming step. In this case, the ligand coordinated to Pd, the pyridone, is non-chiral, so it is very important to elucidate how the chiral induction occur with the norbornene, the only chiral reagent present in the reaction. The acquired mechanistic understanding serves as a starting point for designing next generation of chiral norbornene to enable other remote enantioselective C-H activation reactions.

Scheme 5: Proposed mechanism for the reaction of Scheme 2.

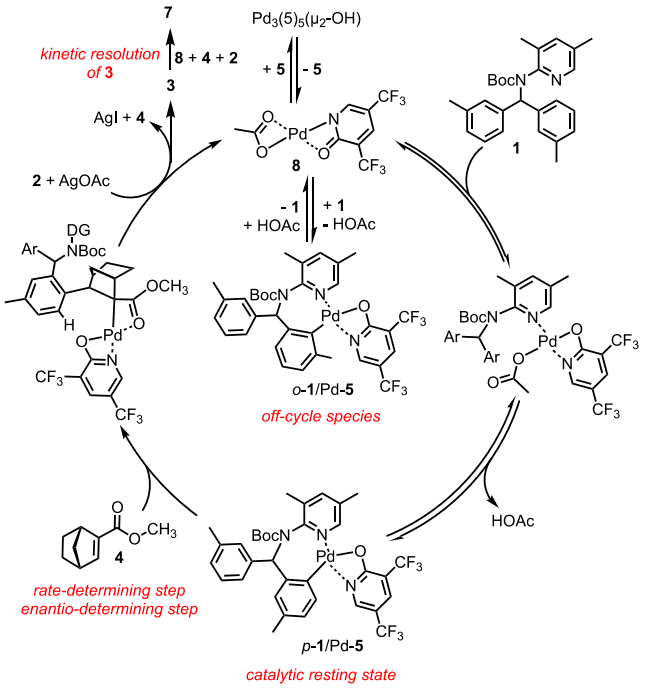

EXPERIMENTAL SECTION

Materials, Analytical Methods, and Instrumentation. ((*R*)-(+)-1-(1-Naphthyl)ethylamine, cis-endo-5-norbornene-2,3-dicarboxylic anhydride, 1,8-diazabicyclo[5.4.0]undec-7-ene, 2-bromo-3,5-dimethylpyridine, 3-bromotoluene, methyl 2,2-difluoro-2-(fluorosulfonyl)acetate, *N*-iodosuccinimide, 2-hydroxy-3-trifluoromethylpyridine, 1-iodo-2-nitrobenzene, and decafluorobiphenyl were purchased from Combi Blocks. Carbon tetrachloride, bromine, 3-methylbenzonitrile, Davephos, sodium *tert*-butoxide, copper(I) iodide, benzyl bromide, silver acetate, diphenyl phosphate, di-tert-butyl-dicarbonate, methyl magnesium bromide, tetrahydrofuran, dimethylformamide, iodine, magnesium turnings, dioxane, and toluene were purchased from Sigma Aldrich. Quinidine, palladium(0) bis(dibenzylideneacetone), lithium aluminum hydride, and triethylamine were purchased from Acros Organics. Mercury(II) oxide (red) and palladium acetate were purchased from Oakwood Chemical. Magnesium sulfate and silica gel 60 F254 plates (20 x 20 cm) were purchased from EMD Millipore Corporation. Hexanes, ethyl acetate, pentane, methylene chloride, and chloroform were purchased from Fischer Scientific. Potassium carbonate was purchased from Aqua Solutions Inc. 10% Palladium on carbon and silica gel 60, 0.032-0.063 mm (230-450 mesh) were purchased from Alfa Aesar. Hydrogen was purchased from Praxair. Chloroform-d_1 (99.8% D) and acetonitrile-d_3 (99.8%

D) were purchased from Cambridge Isotope Laboratories. **1**, **4, 5**, and **8** were prepared according to literature procedure. NMR spectra were acquired on Bruker DRX-600 equipped with a 5 mm DCH cryoprobe, DRX-500, and AMX-400 instruments and calibrated using residual non-deuterated solvent as an internal reference.^{19}F NMR were referenced against a decafluorobiphenyl internal standard and $CFCl_3$ external standard. The following abbreviations (or combinations thereof) are used to explain the multiplicities: s = singlet, d = doublet, t = triplet, q = quartet, m = multiplet, br = broad. Reverse phase HPLC measurements were conducted on either an Agilent 1290 Infinity II HPLC equipped with a C18 column and DAD detector or a Waters I Class HPLC equipped with a C18 column and DAD detector. Normal Phase Chromatography measurements were conducted on either an Agilent 1100 equipped with a DAD detector or a Waters UPC2 SFC equipped with a DAD detector.

Procedure for the Synthesis of tert-butyl(bis(5-methyl-2'-nitro-[1,1'-biphenyl]-3-yl)methyl)(3,5-dimethylpyridin-2-yl)carbamate (**7**) To a 10 mL biotage microwave vial was added **1** (30. mg, 0.072 mmol), **2** (81. mg, 0.353 mmol), silver acetate (50. mg, 0.300 mmol), palladium acetate (4.3 mg, 0.019 mmol), **5** (3.3 mg, 0.014 mmol), **4** (11.1 mg, 0.073 mmol), chloroform (1 mL), and a magnetic stir bar. The vial was capped and then placed in an oil bath heated to 80 °C for 17 hours. After cooling to ambient temperature, the reaction mixture was filtered through Celite and eluted with ethyl acetate. The filtrate was evaporated under reduced pressure. The crude material was chromatographed with silica chromatography (20% ethyl acetate in hexanes) to yield **7** (37 mg, 0.056 mmol, 78% yield) as a yellow-orange solid. ^{1}H NMR (600 MHz, Chloroform-*d*) δ 8.11 (s, 1H), 7.80 (dd, *J* = 24.6, 8.1 Hz, 2H), 7.73 (s, 1H), 7.59 – 7.51 (m, 2H), 7.49 – 7.37 (m, 4H), 7.24 (s, 1H), 7.14 (s, 1H), 7.03 (s, 1H), 7.00 (s, 1H), 6.91 (s, 1H), 6.81 (s, 1H), 6.50 (s, 1H), 2.38 (s, 3H), 2.21 (s, 5H), 1.98 (s, 3H), 1.28 (s, 9H). ^{13}C{^{1}H} NMR (151 MHz, $CDCl_3$) δ 153.6, 149.9, 149.0, 148.6, 145.8, 141.6, 139.1, 137.5, 137.0, 136.6, 136.5, 136.2, 135.9, 131.7, 131.6, 131.5, 130.8, 130.4, 128.6, 127.4, 126.8, 126.6, 126.3, 124.9, 123.6, 123.4, 80.2, 66.1, 27.7, 21.1, 20.7, 17.3, 17.0 HRMS (ESI-TOF) *m*/*z* calculated for $C_{39}H_{39}N_4O_6$ $[M+H]^+$: 659.2870; found: 659.2878.

*Procedure for the Synthesis of tert-butyl (3,5-dimethylpyridin-2-yl)((5-fluoro-2'-nitro-[1,1'-biphenyl]-3-yl)(3-fluorophenyl)methyl)carbamate (***3-F***).* To a 10 mL biotage microwave vial was added **1-F** (43. mg, 0.10 mmol), **2** (68. mg, 0.297 mmol), silver acetate (45. mg, 0.270 mmol), palladium acetate (3.2 mg, 0.014 mmol), **5** (3.9 mg, 0.0169 mmol), **4** (9.2 mg, 0.061 mmol), chloroform (1 mL), and a magnetic stir bar. The vial was capped and then placed in an oil bath heated to 80 °C for 17 hours. After cooling to ambient temperature, the reaction mixture was filtered through Celite and eluted with ethyl acetate. The filtrate was evaporated under reduced pressure. The crude material was chromatographed with silica chromatography (20% ethyl acetate in hexanes) to yield **3-F** (30 mg, 0.055 mmol, 55% yield) as a yellow solid. **3-F** presents as a mixture containing rotomers which complicated characterization by NMR. ^{1}H NMR (600 MHz, $CDCl_3$) δ 8.29, 8.28, 8.23, 8.22, 8.03, 8.02, 8.01, 7.87, 7.72, 7.71, 7.70, 7.69, 7.62, 7.61, 7.60, 7.59, 7.54, 7.50, 7.49, 7.49, 7.45, 7.32, 7.20, 7.13, 7.10, 6.69, 6.87, 6.81, 6.77, 6.51, 2.22, 2.00, 1.29. ^{13}C{^{1}H} NMR (151 MHz, $CDCl_3$) δ 153.9, 150.2, 149.3, 149.0, 146.5, 144.5, 143.6, 141.4, 139.9, 139.7, 135.7, 135.2, 134.4, 134.2, 133.2, 132.5, 132.4, 132.1, 131.9, 131.2, 129.7, 129.6, 129.3, 128.8, 125.7, 125.3, 124.9, 124.4, 124.2, 123.3, 117.0, 115.6, 114.2, 81.3, 66.0, 28.2, 17.9, 17.6. ^{19}F NMR (376 MHz, Chloroform-*d*, 25 °C) δ -113.44 (dd, *J* = 181.5, 118.8 Hz). ^{19}F NMR (376 MHz, Chloroform-*d*, 50 °C) δ -113.31 (d, *J* = 147.8 Hz). HRMS (ESI-TOF) *m*/*z* calculated for $C_{31}H_{30}F_2N_3O_4$ $[M+H]^+$: 546.2204; found: 546.2198.

*Procedure for the Synthesis of tert-butyl (bis(5-fluoro-2'-nitro-[1,1'-biphenyl]-3-yl)methyl)(3,5-dimethylpyridin-2-yl)carbamate (***7-F***).* To a 10 mL biotage microwave vial was added **1-F** (43. mg, 0.10 mmol), **2** (68. mg, 0.297 mmol), silver acetate (45. mg, 0.270 mmol), palladium acetate (3.2 mg, 0.014 mmol), **5** (3.9 mg, 0.0169 mmol), **4** (9.2 mg, 0.061 mmol), chloroform (1 mL), and a magnetic stir bar. The vial was capped and then placed in an oil bath heated to 80 °C for 17 hours. After cooling to ambient temperature, the reaction mixture was filtered through Celite and eluted with ethyl acetate. The filtrate was evaporated under reduced pressure. The crude material was chromatographed with silica chromatography (20% ethyl acetate in hexanes) to yield **7-F** (8 mg, 0.012 mmol, 12% yield) as an off-white solid. **7-F** presents as a mixture containing rotomers which complicated characterization by NMR. ^{1}H NMR (600 MHz, $CDCl_3$) δ 8.08, 7.86, 7.59, 7.50, 7.48, 7.25, 6.96, 6.92, 6.87, 6.76, 6.54, 2.21, 2.02, 1.30. ^{13}C{^{1}H} NMR (151 MHz, CDCl3) δ 163.7, 162.8, 162.0, 161.2, 153.9, 149.8, 19.2, 148.8, 146.5, 144.2, 141.8, 139.9, 139.3, 139.1, 135.6, 135.1, 132.6, 132.5, 132.1, 132.0, 131.3, 128.7, 125.6, 124.4, 124.0, 116.9, 115.6, 115.4, 114.4, 114.3, 114.1, 113.9, 81.4, 66.0, 65.8, 60.5, 31.0, 29.8, 28.2, 17.9, 17.5, 15.4, 14.3, 14.2. ^{19}F NMR (376 MHz, Chloroform-*d*, 25 °C) δ -112.80, -113.41.^{19}F NMR (376 MHz, Chloroform-*d*, 50 °C) δ -113.53. HRMS (ESI-TOF) *m*/*z* calculated for $C_{37}H_{33}F_2N_4O_6$ $[M+H]^+$: 667.2368; found: 667.2365.

General Kinetics Procedure. To a 5 mL volumetric flask was added **4** (30.4 mg, 0.20 mmol) and **5** (34.7 mg, 0.15 mmol). The contents of the 5 mL volumetric flask were dissolved in chloroform using sonication to prepare a **4**/**5**–stock solution ([**5**] = 0.04 M, [**4**] = 0.03 M). To a separate 5 mL volumetric flask was added palladium acetate (22.5 mg, 0.10 mmol) and decafluorobiphenyl (167.1 mg, 0.50 mmol). The contents of this Pd/decafluorobiphenyl volumetric flask were dissolved in chloroform using sonication to prepare a palladium/decafluorobiphenyl–stock solution ([$Pd(OAc)_2$] = 0.02 M, [decafluorobiphenyl] = 0.10 M).

To a kinesis microwave reaction vial (0.5-2mL) with conical stir bar was added silver acetate (54. mg, 0.3 mmol), **2** (68.4 mg, 0.3 mmol), **1** (42.3 mg, 0.10 mmol), and **4**/**5**–stock solution (500 µL). The microwave vial was capped, placed in an oil bath preheated to 80 °C, and left mixing for 3 minutes, then after this time the palladium/ decafluorobiphenyl–stock solution (500 µL) was added to start the reaction. Aliquots (~ 20 microliters) of the reaction mixture were taken using a new hypodermic needle affixed to a 1mL disposable syringe, quenched into methanol (1 mL), and then purified through syringe filter (PTFE, 0.45 µm). The aliquot was analyzed by RP-HPLC to determine concentration of each analyte of interest and by RP-HPLC-SFC 2-dimensional chromatography to determine the % *e.e.* of **3**.

AUTHOR INFORMATION

Corresponding Author

* E-mail: blackmond@scripps.edu

ORCID

0000-0001-9829-8375 (D.G.B)
0000-0003-3560-5774 (J.-Q.Y.)
0000-0002-7326-2509 (D.E.H.)

Notes

The authors declare no competing financial interest.

‡Present address: The Warren and Katharine Schlinger Laboratory for Chemistry and Chemical Engineering, Division of Chemistry and Chemical Engineering, California Institute of Technology, Pasadena, California 91125 USA

SUPPORTING INFORMATION

Details of experimental procedures, full kinetic data, NMR data.

ACKNOWLEDGMENT

This is work was supported by the National Science Foundation under the Center for Chemical Innovation Center for Selective C−H Functionalization (CHE-1700982) and by the Centre for Rapid Online Analysis of Reactions (ROAR) at Imperial College London [EPSRC, EP/R008825/1]. Dr. Jason Chen, Brittaney Sanchez, and Emily Strugell of the Scripps Automated Synthesis Center are acknowledged for valuable guidance and support on analytical methods. Prof. Mimi Hii, Dr. Benjamin Deadman, and Dr. Paola Ferrini are acknowledged for helpful discussion and support on analytical methods.

REFERENCES

1. Wang, P.; Farmer, M. E.; Huo, X.; Jain, P.; Shen, P.-X.; Ishoey, M.; Bradner, J. E.; Wisniewski, S. R.; Eastgate, M. D.; Yu, J.-Q., Ligand-Promoted *meta*-C–H Arylation of Anilines, Phenols, and Heterocycles. *J. Am. Chem. Soc.* **2016,** *138*, 9269-9276.

2. Wang, P.; Li, G.-C.; Jain, P.; Farmer, M. E.; He, J.; Shen, P.-X.; Yu, J.-Q., Ligand-Promoted *meta*-C–H Amination and Alkynylation. *J. Am. Chem. Soc.* **2016,** *138*, 14092-14099.

3. Shi, H.; Wang, P.; Suzuki, S.; Farmer, M. E.; Yu, J.-Q., Ligand Promoted *meta*-C–H Chlorination of Anilines and Phenols. *J. Am. Chem. Soc.* **2016,** *138*, 14876-14879.

4. Li, G.-C.; Wang, P.; Farmer, M. E.; Yu, J.-Q., Ligand-Enabled Auxiliary-Free *meta*-C−H Arylation of Phenylacetic Acids. *Angew. Chem. Int. Ed.* **2017,** *56*, 6874-6877.

5. Wang, P.; Verma, P.; Xia, G.; Shi, J.; Qiao, J. X.; Tao, S.; Cheng, P. T. W.; Poss, M. A.; Farmer, M. E.; Yeung, K.-S.; Yu, J.-Q., Ligand-Accelerated Non-Directed C–H Functionalization of Arenes. *Nature.* **2017,** *551*, 489.

6. Zhu, R.-Y.; Li, Z.-Q.; Park, H. S.; Senanayake, C. H.; Yu, J.-Q., Ligand-Enabled γ-C(sp^3)–H Activation of Ketones. *J. Am. Chem. Soc.* **2018,** *140*, 3564-3568.

7. Shi, H.; Herron, A. N.; Shao, Y.; Shao, Q.; Yu, J.-Q., Enantioselective Remote *meta*-C–H Arylation and Alkylation via a Chiral Transient Mediator. *Nature.* **2018,** *558*, 581-585.

8. Farmer, M. E.; Wang, P.; Shi, H.; Yu, J.-Q., Palladium-Catalyzed *meta*-C–H Functionalization of Masked Aromatic Aldehydes. *ACS Catal.* **2018,** *8*, 7362-7367.

9. Liu, L.-Y.; Yeung, K.-S.; Yu, J.-Q., Ligand-Promoted Non-Directed C−H Cyanation of Arenes. *Chem. Eur. J.* **2019,** *25*, 2199-2202.

10. Wang, J.; Dong, G., Palladium/Norbornene Cooperative Catalysis. *Chem. Rev.* **2019,** *119*, 7478-7528.

11. Catellani, M.; Motti, E.; Della Ca', N., Catalytic Sequential Reactions Involving Palladacycle-Directed Aryl Coupling Steps. *Acc. Chem. Res.* **2008,** *41*, 1512-1522.

12. Blackmond, D. G., Reaction Progress Kinetic Analysis: A Powerful Methodology for Mechanistic Studies of Complex Catalytic Reactions. *Angew. Chem. Int. Ed.* **2005,** *44*, 4302-4320.

13. Mathew, J. S.; Klussmann, M.; Iwamura, H.; Valera, F.; Futran, A.; Emanuelsson, E. A. C.; Blackmond, D. G., Investigations of Pd-Catalyzed ArX Coupling Reactions Informed by Reaction Progress Kinetic Analysis. *J. Org. Chem.* **2006,** *71*, 4711-4722.

14. Burés, J., A Simple Graphical Method to Determine the Order in Catalyst. *Angew. Chem. Int. Ed.* **2016,** *55*, 2028-2031.

15. Ball, N. D.; Kampf, J. W.; Sanford, M. S., Aryl−CF3 Bond-Forming Reductive Elimination from Palladium(IV). *J. Am. Chem. Soc.* **2010,** *132*, 2878-2879.

16. Scharf, A.; Goldberg, I.; Vigalok, A.; Vedernikov, A. N., Aryl–F Bond Cleavage vs. C–E Reductive Elimination: Competitive Pathways of Metal–Ligand-Cooperation-Based E–H Bond Activation (E = N, S). *European Journal of Inorganic Chemistry.* **2015,** *2015*, 4761-4768.

17. Neukom, J. D.; Perch, N. S.; Wolfe, J. P., Intramolecular Insertion of Alkenes into Pd−N Bonds. Effects of Substrate and Ligand Structure on the Reactivity of (P−P)Pd(Ar)[$N(Ar_1)(CH_2)_3CR{=}CHR'$] Complexes. *Organometallics.* **2011,** *30*, 1269-1277.

18. Carrow, B. P.; Hartwig, J. F., Ligandless, Anionic, Arylpalladium Halide Intermediates in the Heck Reaction. *J. Am. Chem. Soc.* **2010,** *132*, 79-81.

19. Thomas, A. A.; Wang, H.; Zahrt, A. F.; Denmark, S. E., Structural, Kinetic, and Computational Characterization of the Elusive Arylpalladium(II)boronate Complexes in the Suzuki–Miyaura Reaction. *J. Am. Chem. Soc.* **2017,** *139*, 3805-3821.

20. Sgro, M. J.; Stephan, D. W., Ni(II), Pd(II) and Pt(II) complexes of PNP and PSP tridentate amino–phosphine ligands. *Dalton Transactions.* **2012,** *41*, 6791-6802.

21. Jia, F.; Luo, J.; Zhang, B. Mechanistic Insight into Palladium-Catalyzed Enantioselective Remote *meta*-C-H Arylation and Alkylation by Using Density Functional Theory (DFT) Calculations. *Adv. Synth. Catal.* **2020**, *362*, 1686-1695.

22. Shi, H.; Herron, A. N.; Shao, Y.; Shao, Q.; Yu, J.-Q. Enantioselective remote meta-C-H arylation and alkylation via a chiral transient mediator. *Nature* **2018**, *558*, 581-585.

TOC Graphic

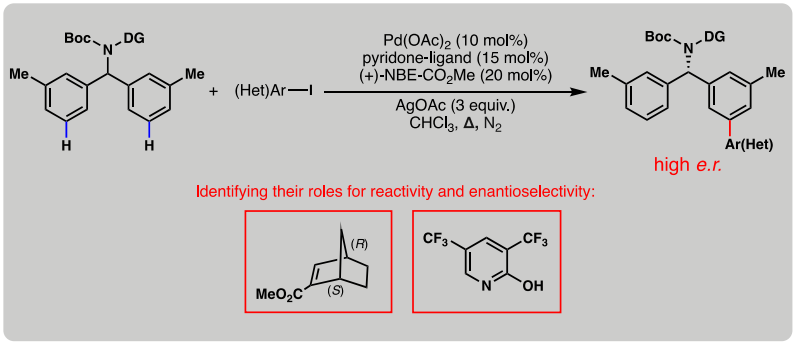
Boc
N
DG
Me
Me
H
H
+ (Het)Ar—I
Pd(OAc)2 (10 mol%)
pyridone-ligand (15 mol%)
(+)-NBE-CO2Me (20 mol%)
AgOAc (3 equiv.)
CHCl3, Δ, N2
Boc
N
DG
Me
Me
Ar(Het)
high e.r.
Identifying their roles for reactivity and enantioselectivity:
(R)
(S)
MeO2C
CF3
CF3
N
OH